Available online at www.sciencedirect.com
ScienceDirect
Journal of Magnetic Resonance 187 (2007) 131–140
JMR Journal of Magnetic Resonance
www.elsevier.com/locate/jmr

First principles NMR calculations of phenylphosphinic acid $C_6H_5HPO(OH)$: Assignments, orientation of tensors by local field experiments and effect of molecular motion

C. Gervais [a,*], C. Coelho [a], T. Azaïs [a], J. Maquet [a], G. Laurent [a], F. Pourpoint [a], C. Bonhomme [a,*], P. Florian [b], B. Alonso [c], G. Guerrero [d], P.H. Mutin [d], F. Mauri [e]

[a] *Université Pierre et Marie Curie-Paris 6, UMR 7574 Laboratoire de Chimie de la Matière Condensée de Paris, Paris F-75005, France*
[b] *CRMHT CNRS, 1D avenue de la Recherche Scientifique, 45071 Orléans Cedex 2, France*
[c] *Institut Charles Gerardt, UMR 5223 CNRS-UM2-ENSCM-UM1, MACS, 8 rue de l'Ecole Normale, 34296 Montpellier Cedex 5, France*
[d] *Institut Charles Gerardt, UMR 5223 CNRS-UM2-ENSCM-UM1, Chimie Moléculaire et Organisation du Solide, Université de Montpellier 2, CC007, Place Eugène Bataillon 34095 Montpellier Cedex 5, France*
[e] *Université Pierre et Marie Curie-Paris 6, UMR 7590 Laboratoire de Minéralogie-Cristallographie de Paris, Paris F-75005, France*

Received 12 February 2007; revised 19 March 2007
Available online 7 April 2007

Abstract

The complete set of NMR parameters for ^{17}O enriched phenylphosphinic acid $C_6H_5HP_*O(^*OH)$ is calculated from first principles by using the Gauge Including Projected Augmented Wave (GIPAW) approach [C.J. Pickard, F. Mauri, All-electron magnetic response with pseudopotentials: NMR chemical shifts, Phys. Rev. B 63 (2001) 245101/1–245101/13]. The analysis goes beyond the successful assignment of the spectra for all nuclei (^1H, ^{13}C, ^{17}O, ^{31}P), as: (i) the ^1H CSA (chemical shift anisotropy) tensors (magnitude and orientation) have been interpreted in terms of H bonding and internuclear distances. (ii) CSA/dipolar local field correlation experiments have allowed the orientation of the direct P–H bond direction in the ^{31}P CSA tensor to be determined. Experimental and calculated data were compared. (iii) The overestimation of the calculated ^{31}P CSA has been explained by local molecular reorientation and confirmed by low temperature static $^1H \rightarrow {}^{31}P$ CP experiments.

Keywords: Solid state NMR; ^1H CSA; GIPAW calculations; Tensors

1. Introduction

The PAW (Projector Augmented Wave) and GIPAW (Gauge Including Projected Augmented Wave) methods have attracted recently much attention in the field of solid state NMR [1]. Accurate predictions of isotropic chemical shifts and quadrupolar constants have been achieved for model organic/bioorganic [2] and inorganic [3] compounds. These compounds include molecular crystals, as well as 3D architectures. The success of both methods relies on the fact that large infinite solids are described within periodic boundary conditions, using plane wave basis sets and Density Functional Theory (DFT). It follows that the only significant source of error is the use of approximated exchange-correlation DFT functionals.

As a matter of fact, the proposed first principles calculations lead to numerous NMR parameters, allowing deep insight in the description of crystal structures. It is therefore possible *to go beyond the crude assignment of isotropic lines in a given spectrum*. Among these parameters, calculated CSA parameters have been reported. To the best of our knowledge, only *isotropic* GIPAW calculated ^1H shifts have been proposed in the literature for a limited number of derivatives [2b,2c,4,5]. Surprisingly, GIPAW calculated

* Corresponding authors. Fax: +33 1 44 27 47 69.
E-mail addresses: gervais@ccr.jussieu.fr (C. Gervais), bonhomme@ccr.jussieu.fr (C. Bonhomme).

1090-7807/$ - see front matter © 2007 Elsevier Inc. All rights reserved.
doi:10.1016/j.jmr.2007.03.018

^{1}H *CSA* have been rarely reported [6], though precise data based on single crystal experiments have been published already [7]. At this stage, we must mention that recent work by Haeberlen and coworkers reported ^{1}H calculated data in the frame of a spherical cluster approach, with no periodic boundary conditions [8]. Proton *ab initio* calculations were initiated by McMichael Rolfing [9] in the frame of ROH molecules and carboxylic acid dimers.

The absolute orientation of the principal axes of all tensors is also calculated within the GIPAW approach, opening a new field of research. Experiments on single crystals [8a,10] and static powders allow in principle the determination of the orientation of tensors. As an example, the orientations of CSA and quadrupolar tensors have been previously reported in the case of 1D ^{17}O, ^{55}Mn, ^{95}Mo and ^{139}La static spectra [2b,11,12] and compared to first principles calculations. In this particular case, the discontinuities of the spectra were characteristic for both the magnitude and relative orientation of the corresponding tensors. Several solid state NMR correlation experiments have been proposed in the literature [13] allowing the relative orientations of various tensors (CSA, dipolar, quadrupolar) to de determined. The aim of this article is to show that correlation experiments can be effectively combined with GIPAW calculations. It has to be noticed that van Beek et al. [13c] have recently used GIPAW tensorial data for simulation purposes.

It is well established that local molecular motion may average (at least partially) the NMR interactions. It follows that the observed experimental parameters can be strongly modulated in terms of anisotropy and orientation of the principal axes. This crucial notion is rarely addressed in the literature though the PAW and GIPAW calculations are performed actually at 0 K (a notable exception is a recent contribution by Rossano et al. [14]); thus, care must be taken when comparing experimental and calculated data. On the other hand, discrepancies between experimental and calculated data *may suggest* the presence of local molecular motion.

The PAW and GIPAW methods lead also to interesting data, which open new perspectives in solid state NMR: (a) the absolute value of C_Q could be of great help in the frame of NQR spectroscopy, by specifying the resonance frequencies. Moreover, the sign of C_Q is also provided by the PAW approach. (b) the *antisymmetric* components of the tensors are calculated as well; very little attention has been paid so far to these components [7a] but recent work by Wi and Frydman [15] demonstrated their potential in solid state NMR.

In this paper, the PAW and GIPAW methods are applied to the fine description of the NMR parameters of ^{17}O enriched phenyl*phosphinic* acid, $C_6H_5HP^*O(^*OH)$. This derivative is characterized by a direct P–H bond. Organophosphorus derivatives, such as phenyl*phosphonic* or phenyl*phosphinic* acids, are interesting for the synthesis of hybrid materials [16] and titano- or aluminophosphonate(inate) clusters [17,18]. Solid state NMR is an invaluable tool of investigation for such organophosphorus derived materials, giving a deep insight into chemical bonding. As an example, it has been shown recently [19] that ^{17}O parameters were extremely sensitive to the bonding mode of phosphonate molecules in hybrid solids. Here, we find a very good agreement between the experimental and calculated data for all nuclei (^{1}H, ^{13}C, ^{17}O, ^{31}P) of phenyl*phosphinic* acid, confirming results dealing with a *phosphonic* derivative, $C_6H_5PO(OH)_2$ [5]. In the case of this *phosphonic* derivative, the calculated ^{1}H data were not discussed. In the present work, the analysis of the calculated data includes the following points: (i) ^{1}H data (including the CSA and the orientation of the corresponding tensors) have been interpreted in terms of H bonding and internuclear distances. The proposed discussion includes ^{1}H data related to phenyl*phosphinic* and phenyl*phosphonic* acids, various hydrated calcium phosphates exhibiting P–OH groups ($CaHPO_4{\cdot}2H_2O$, $Ca(H_2PO_4)_2{\cdot}H_2O$) and hydroxyapatite (HAp), $Ca_5(PO_4)_3(OH)$ [6]. (ii) The dipolar tensor corresponding to the direct P–H bond was oriented in the ^{31}P CSA tensor using a dipolar mediated correlation experiment (Inversion Recovery Cross Polarization or IRCP) [20]. Extensive use of the SIMPSON simulation platform [21] allowed the interpretation of the data. (iii) The overestimation of the *calculated* ^{31}P CSA was explained by local molecular reorientation. Low temperature experiments confirmed this assumption.

The outline of the article is the following: Section 2 presents the Experimental details (synthesis of the ^{17}O enriched phenylphosphinic acid and solid state NMR experiments at low and room temperature). Section 3 deals with the Computational details, including the first principles calculations and the SIMPSON simulation approach. Section 4 presents both calculated and experimental results.

2. Experimental details

2.1. Synthesis of ^{17}O enriched phenylphosphinic acid, $C_6H_5HP^*O(^*OH)$

Dichlorophenyl phosphine ($PhPCl_2$, 97%, Aldrich) was distilled under reduced pressure before use. $PhPCl_2$ (2.52 g, 14.1 mmol) was slowly added to enriched water (20 at. %, 0.77 g, 42.2 mmol) in dry THF (6 mL) at 0 °C. The reaction mixture was stirred for 30 min at this temperature, then warmed at room temperature and argon was bubbled overnight into the solution to remove dissolved hydrogen chloride. After evaporation, the white solid was recrystallized from acetonitrile solutions to give white crystals (1.50 g, 74%). Phenylphosphinic acid (non ^{17}O enriched) was purchased from Aldrich and studied without further purification.

2.2. Multinuclear solid state NMR

^{1}H NMR MAS spectra were obtained at 750.16 MHz (17.6 T) using a 2.5 mm Bruker probe (MAS frequency: 33 kHz) (Bruker AVANCE 750 spectrometer, number of

scans: 4, 30° pulse with $\omega(^1H)/2\pi = 50.0$ kHz for full relaxation). Spectra were referenced to TMS.

$^1H \rightarrow {}^{13}C$ CP MAS experiments were performed at 75.43 MHz (7.0 T) (Bruker AVANCE 300 spectrometer) using a 4 mm Bruker probe at 5 kHz. ($\omega(^1H)/2\pi = 46.3$ kHz during the contact time (2 ms), number of scans: 832, relaxation delay: 20 s, ^1H TPPM composite decoupling [22], 15°, decoupling power of 50 kHz). Spectra were referenced to TMS.

$^1H \rightarrow {}^{31}P$ CP and IRCP [20] experiments were performed at 121.44 MHz (7.0 T) using a 4 mm Bruker probe. Both static and MAS (5 kHz) modes were used (in static mode: $\omega(^1H)/2\pi = \omega(^{31}P)/2\pi = 58.1$ kHz during the contact time (3 ms), number of scans: 704, relaxation delay: 20 s). Spectra were referenced to H_3PO_4, 85%. For the IRCP sequence (see Fig. 6c), a sudden inversion of phase on the ^{31}P channel is applied after the initial CP contact (3 ms). In order to record undistorted ^{31}P static lineshapes, a final π pulse was added (in order to form an echo). Static $^1H \rightarrow {}^{31}P$ CP experiments (including an echo) were also performed at low temperature ($T = -40$ °C) by using the air driven Bruker BCU-Extreme apparatus and a triple resonance DVT Bruker probe. The pressure dew point of the drier (Bruker) was −100 °C. The temperature has been carefully calibrated by using solid lead nitrate (the ^{207}Pb chemical shift is a sensitive temperature sensor) [23].

^{17}O MAS and static NMR spectra were recorded at 54.22 (9.4 T) and 101.69 MHz (17.6 T) (Bruker AVANCE 400 and 750 spectrometers) using Bruker 4 mm probes. Static spectra were acquired using a spin-echo (θ–τ–2θ) pulse sequence with $\theta = 90°$ (on the solid) to overcome problems of probe ringing and baseline distortions while at 17.6 T, the ^{17}O MAS (12.5 kHz) spectrum was recorded using a single-pulse excitation with a short ($<\pi/16$) pulse, since only a very short pre-acquisition delay was needed (^1H TPPM composite decoupling, 20°, decoupling power of 50 kHz, relaxation delay: 5 s, number of scans: 25,000–200,000). Chemical shifts were referenced to tap water ($\delta = 0$ ppm).

3. Computational details

3.1. The GIPAW approach

The calculations were performed within the Kohn–Sham DFT using the PARATEC code [24]. Full details related to the implementation of the PAW and GIPAW methods are given in Ref. [5]. The crystalline structure is described as an infinite periodic system using periodic boundary conditions. The NMR calculations are performed as follows: partial geometry optimizations were performed for the structure, starting with the experimental structure [25] and allowing the positions of the hydrogen and carbon atoms to relax using DFT calculation. It has been shown previously [5] in the case of phenyl*phosphonic* acid that net improvement in the calculations of both ^1H and ^{13}C resonances was obtained by relaxing proton and carbon positions (in the case of single crystal XRD data). We have shown here that all ^{13}C resonances were systematically deshielded by considering the sole relaxation of protons (in the case of the phenyl*phosphinic* acid). The new coordinates obtained after relaxation are summarized in Supporting Information. Representation of one phenyl*phosphinic* acid molecule showing the labelling scheme of the atoms and H-bonding scheme are presented in Fig. 1. The schematic representation of one phenyl*phosphonic* acid molecule is also presented in Fig. 1 for further discussion. The shielding tensor was computed using the GIPAW approach [1,26] which permitted the reproduction of the results of a fully converged all-electron calculation while the EFG tensors were computed using a PAW approach [27,28]. The isotropic chemical shift δ_{iso} is defined as $\delta_{iso} = -(\sigma - \sigma^{ref})$, where σ is the isotropic shielding (one-third of the trace of the NMR shielding tensor) and σ^{ref} is the isotropic shielding of the same nucleus in a reference system as previously described in Ref. [5]. The values given in Ref. [5] and used in this work are the following: $\sigma^{ref}(^1H) = 31.0$ ppm, $\sigma^{ref}(^{13}C) = 170.9$ ppm,

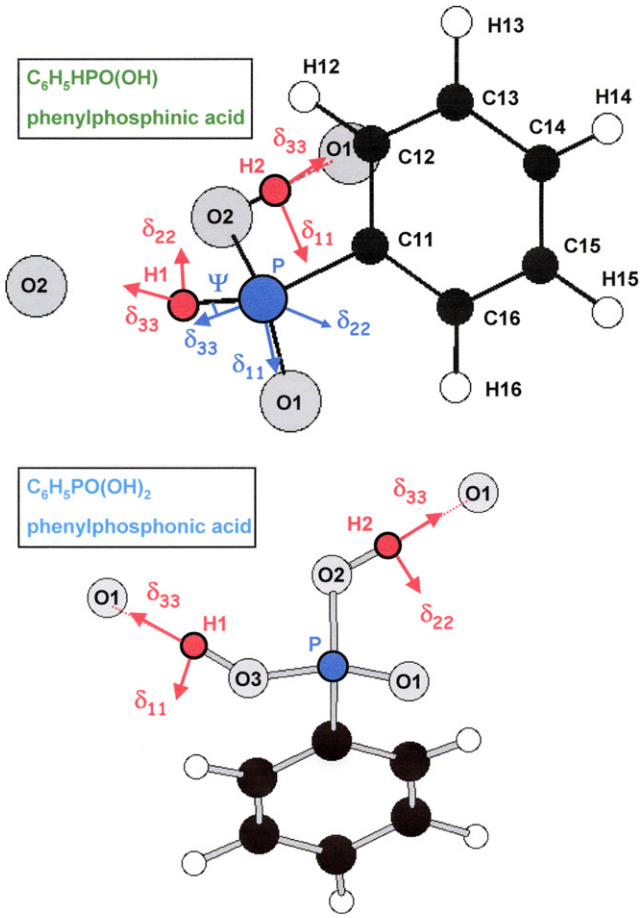

Fig. 1. Representation of $C_6H_5HPO(OH)$ and $C_6H_5PO(OH)_2$ molecules, showing the labelling scheme of the atoms. The ^{31}P and ^1H CSA principal axes obtained from the calculations are represented by δ_{11}, δ_{22} and δ_{33}. Red dashed lines, H-bonding directions. Ψ, angle between δ_{33} (^{31}P) and the P–H direction. (For interpretation of the references to color in this figure legend, the reader is referred to the web version of this paper.)

$\sigma^{ref}(^{31}P) = 300.7$ ppm and $\sigma^{ref}(^{17}O) = 261.5$ ppm. All calculated and experimental NMR data are reported in Tables 1 and 2.

3.2. SIMPSON simulations

The simulations of spectra presented in the work were performed by using the DM2004 program [29] and the SIMPSON platform [21]. Both programs are available on the web. In the frame of SIMPSON, the MAS simulations were performed by using the *g-compute* method. *γ-angles* and *crystal-file* were adapted to obtain the convergence of the simulations. In the case of ^{17}O, the quadrupolar interaction was considered up to the second-order. The I_{1c} and I_{1p} input were used in order to obtain the central transition (CT) and the satellite transitions (ST), respectively. For all nuclei, isotropic chemical shift and CSA were used as input parameters. For ^{17}O, Euler angles relating the CSA (δ_{11}, δ_{22}, δ_{33}) and the quadrupolar (C_Q, η_Q) tensors were specified by:

shift	α	β	γ
quadrupole	0	0	0

Definitions of δ_{11}, δ_{22}, δ_{33}, C_Q, η_Q and Euler angles are given in Table 1. The three Euler angles describe the relative orientation of the CSA tensor with respect to the EFG tensor system [2b]. The IRCP simulations were performed by considering $I_{1y} + I_{2y}$ as *start-operator* and I_{2p} as detect-operator (nucleus 1: ^{1}H ; nucleus 2: ^{31}P). The RF during the inversion-time (t_i) and the phases on both channels ($Y, -Y$) were used as input parameters. The ZCW28656 *crystal-file* and the *direct method* were used for static conditions. The orientation of the P–H bond was specified in the ^{31}P CSA tensor by:

dipole	0	β	γ
shift	0	0	0

4. Results and discussion

At very high field (17.6 T) and very high MAS frequency, a considerable gain of resolution is attained in ^{1}H solid state NMR [30]. The ^{1}H spectrum of $C_6H_5HPO(OH)$ (Fig. 2a) exhibits two main lines centered at $\delta = 13.6$ ppm and $\delta \approx 7$ ppm, corresponding to P–O<u>H</u> and (P–<u>H</u>, $C_6\underline{H}_5$) resonances, respectively. The obtained resolution is obviously not sufficient to allow any deconvolution of the complex resonance located at $\delta \approx 7$ ppm. The calculated spectrum using the calculated parameters (Table 1) is in good agreement with the experimental one. These parameters correspond to the relaxed structure involving both C and H atoms (see above). The role of the relaxation of the structure is crucial when dealing with ^{1}H isotropic chemical shifts [2b,5], strengthening the role of H-bonding in the calculations of chemical shifts. For example, the GIPAW method leads to δ(P–O<u>H</u>) = 5.5 ppm before relaxation of the structure and to δ(P–O<u>H</u>) = 13.9 ppm after relaxation. The experimental value of δ(P–O<u>H</u>)

Table 1
^{1}H, ^{13}C, ^{17}O and ^{31}P GIPAW isotropic and anisotropic parameters for $C_6H_5HPO(OH)$

		δ_{iso}	δ EXP	δ_{11}	δ_{22}	δ_{33}	C_Q	EXP	η_Q	EXP	α	β	γ
H1	PH	7.3	[a]	9.1	8.8	4.1							
H2	OH	13.9	13.6	25.9	25.4	−9.5							
H12	Ph	5.8		9.1	6.2	2.2							
H13	Ph	5.3		8.4	5.3	2.1							
H14	Ph	7.1		9.3	7.7	4.3							
H15	Ph	6.1		8.6	7.3	2.5							
H16	Ph	5.2		1.9	4.6	9.1							
C11	C–P	130.5	[a]	218.8	160.9	11.9							
C12	*o*-Ph	132.7		241.8	160.0	−3.6							
C13	*m*-Ph	129.6		239.3	156.4	−6.9							
C14	*p*-Ph	135.6	135.1	246.8	165.0	−5.1							
C15	*m*-Ph	131.7		241.7	157.9	−4.6							
C16	*o*-Ph	132.4		241.1	164.3	−8.1							
O1	P=O	91.8	90.9[b]	146.1	119.9	9.4	−4.67[d]	4.5[b]	0.41	0.44[b]	−95	105	70
O2	OH	85.6	85.7[b]	47.7	68.5	140.6	−6.28[d]	6.1[b]	0.71	0.70[b]	55	75	−120
P		20.1	19.7	−84.2[c]	18.3[c]	126.2[c]							

The experimental data correspond to EXP. δ in ppm, C_Q in MHz and Euler angles in °. CSA, δ_{11}, δ_{22}, δ_{33} with: $|\delta_{33} - \delta_{iso}| \geqslant |\delta_{11} - \delta_{iso}| \geqslant |\delta_{22} - \delta_{iso}|$ and $\delta_{iso} = 1/3\ (\delta_{11}+\delta_{22}+\delta_{33})$. EFG, V_{XX}, V_{YY}, V_{ZZ} with $|V_{ZZ}| \geqslant |V_{XX}| \geqslant |V_{YY}|$ and $C_Q = eQV_{ZZ}/h$, $\eta_Q = (V_{YY} - V_{XX})/V_{ZZ}$. The Euler angles (α, β, γ) describe the relative orientation of the CSA tensor with respect to the EFG tensor [2b]. Experimental $\delta(^{1}H, ^{13}C, ^{31}P) \pm 0.1$ ppm. $\delta\ (^{17}O) \pm 0.5$ ppm. $C_Q\ (^{17}O) \pm 0.1$ MHz, $\eta_Q\ (^{17}O) \pm 0.1$.

o, ortho-; *m*, meta-; *p*, para-.

[a] The spectral resolution was not sufficient to extract all isotropic chemical shifts (see text).

[b] From fast MAS experiment at very high field ($B_0 = 17.6$ T).

[c] The ^{31}P CSA principal components have to be compared to the experimental values: −76.2, 26.6 and 108.9 ppm.

[d] The sign of C_Q is accessible by the calculation.

Table 2
Calculated ^{1}H CSA parameters for the phenyl*phosphinic* and phenyl*phosphonic* acids ($C_6H_5HPO(OH)$, $C_6H_5PO(OH)_2$) and hydroxyapatite HAp ($Ca_5(PO_4)_3OH$) (see Ref. [6])

	$\delta_{iso.}$ (ppm)	δ_{11} (ppm)	δ_{22} (ppm)	δ_{33} (ppm)	dOH···O(Å)
$C_6H_5HPO(OH)$					
H1[a] (PH)	7.3	9.1	8.8	4.1	2.705
H2[a] (POH)	13.9	25.9	25.4	−9.5	1.457
$C_6H_5PO(OH)_2$					
H1[a] (POH)	13.0	25.9	24.7	−11.6	1.536
H2[a] (POH)	11.7	24.3	21.9	−11.0	1.628
$Ca_5(PO_4)_3OH$[b]	−1.5	2.0	1.9	−8.3	[c]

[a] The labelling scheme for the various protons is given in Fig. 1.
[b] The calculations correspond to the monoclinic form of HAp [37].
[c] Isolated OH groups.

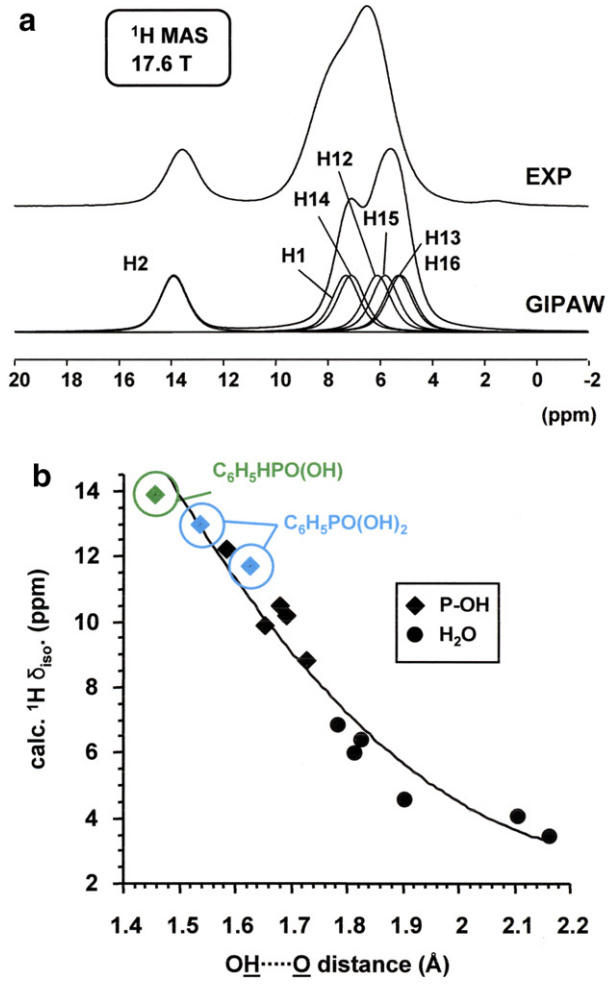

Fig. 2. (a) ^{1}H MAS NMR spectrum (EXP) of $C_6H_5HPO(OH)$. GIPAW: simulation corresponding to the ^{1}H chemical shifts presented in Table 1. (b) Calculated ^{1}H isotropic chemical shifts *vs* the shortest OH···O distances in the corresponding structures for $C_6H_5HPO(OH)$, $C_6H_5PO(OH)_2$ and various hydrated calcium phosphates (namely $CaHPO_4{\cdot}2H_2O$, $Ca(H_2PO_4)_2{\cdot}H_2O$). The solid line is intended as a guideline for the eyes.

(=13.6 ppm) is therefore a good test for the accuracy of the calculations.

Very interestingly, a safe correlation can be established between the calculated ^{1}H *isotropic* chemical shifts and the shortest OH···O distance in the corresponding structures. Fig. 2b presents a compilation of *calculated* data related to OH groups (including P–OH and H_2O molecules) in phenyl*phosphonic* and phenylphosphin*inic* acids, and various hydrated calcium phosphates [6]. A strong deshielding of the ^{1}H isotropic resonance is obviously related to the shortening of the OH···O distance. On this basis, the ^{1}H resonances for both acids are clearly distinguished. This trend is observed for P–OH groups and H_2O molecules, though two different resonance regions have to be considered ($\delta(H_2O) \leqslant 7$ ppm and $\delta(P\text{–}OH) \geqslant 8$ ppm). Empirical correlations leading to analogous conclusions were already published by Berglund and Vaughan [31] and Jeffrey and Yeon [32].

Much more information can be extracted concerning the ^{1}H CSA tensors. Table 2 shows the principal components of the ^{1}H CSA tensors for OH groups in both acids. The corresponding data for HAp ($Ca_5(PO_4)_3OH$) are also presented for comparison: HAp is characterized by "isolated" OH groups in the structure. All tensors corresponding to the acids can be considered as axial, as already observed for several protons involved in H bond networks [7]. Nevertheless, Wu et al. [33] have pointed that ^{1}H CSA tensors can deviate from axial symmetry in the case of crystalline hydrates (including perchlorate and sulfate derivatives). The calculated anisotropy (defined by $|\delta_{33} - \delta_{iso.}|$) is strong (~23 ppm). In the case of HAp, the anisotropy is clearly reduced as isolated OH groups are involved. Moreover, the calculated δ_{33} axis direction is nearly collinear to the OH···O direction for both acids, as anticipated for such OH groups (see Fig. 1). As a matter of fact, the ^{1}H CSA tensor for H1 in the phenyl*phosphinic* acid (P–H bond) is also axial and the unique axis δ_{33} is also nearly collinear to the P–H1···O2 direction. Experimental data concerning direct P–H bonds have not been published so far in the literature. Finally, we note that the calculated ^{1}H CSA for the *aromatic* protons are in agreement with those proposed recently in the case of benzene [8b].

The $^1H \rightarrow {}^{13}C$ CP MAS spectrum of the phenyl*phosphinic* acid is presented in Fig. 3. Calculated data (Table 1) show that the C14(*p*-PH) resonance is expected to be deshielded ($\delta = 135.6$ ppm). The experimental spectrum

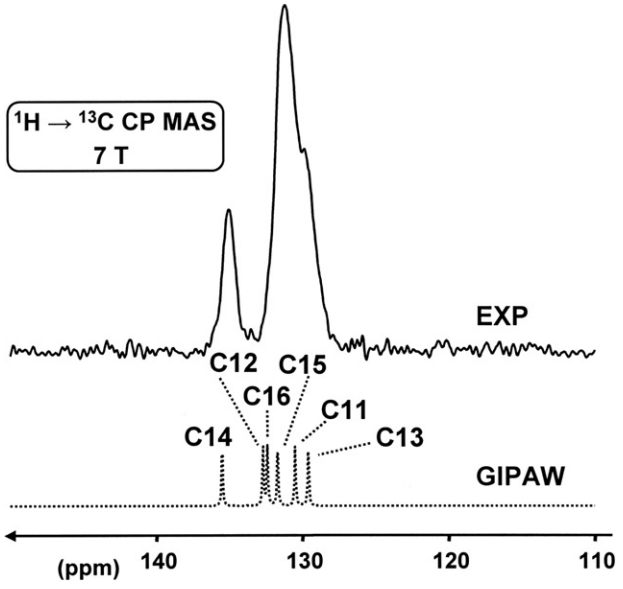

Fig. 3. $^{1}H \rightarrow {}^{13}C$ CP MAS NMR spectrum (EXP) of $C_6H_5HPO(OH)$. GIPAW: ^{13}C isotropic chemical shifts presented in Table 1.

exhibits also a deshielded line at $\delta = 135.1$ ppm which can be safely assigned to C14(*p*-PH). Recently [34], we have proved unambiguously this particular assignment by using $^{1}H \rightarrow {}^{31}P \rightarrow {}^{13}C$ double CP MAS experiments.

Due to second-order quadrupolar broadening [35], it is well known that MAS reorientation of samples can not fully average the broadening of lines corresponding to quadrupolar nuclei (such as ^{17}O, $I = 5/2$). The calculated ^{17}O parameters (including the (α, β, γ) Euler angles between CSA and EFG tensors) are presented in Table 1 for P = O (O1) and P–OH (O2). At 17.6 T, both central transitions (CT) corresponding to O1 and O2 can be almost distinguished and present characteristic features which allow the precise determination of (C_Q, η_Q) for each site (Fig. 4a). By using the calculated parameters, the full ^{17}O MAS spectrum at 17.6 T can be simulated (Fig. 4b). A very good agreement is observed for all CT and satellite transitions features. Under static conditions, CSA parameters and Euler angles between the CSA and quadrupolar tensors can be extracted [2b,11], especially at 17.6 T. The static spectrum at $B_0 = 17.6$ T is well simulated by using the calculated parameters, including the (α, β, γ) Euler angles (Fig. 5a). Fig. 5b shows various calculated lineshapes for O1 and O2. The solid line corresponds to the PAW/GIPAW parameters. The use of other sets of Euler angles ($\alpha = \beta = \gamma = 0°$) for O1 and O2 leads to a completely different lineshape, which can not account for the experimental spectrum. The same conclusion applies when considering no CSA for O1 and O2. Therefore, the relative orientation of the CSA and EFG tensors is of crucial importance, when dealing with the static lineshapes. Spectra obtained at 9.4 T confirm the accuracy of the calculations (Fig. 5c). We note that the trends observed for C_Q [*i.e.* C_Q(P–OH) > C_Q(P=O)] are in agreement with previously

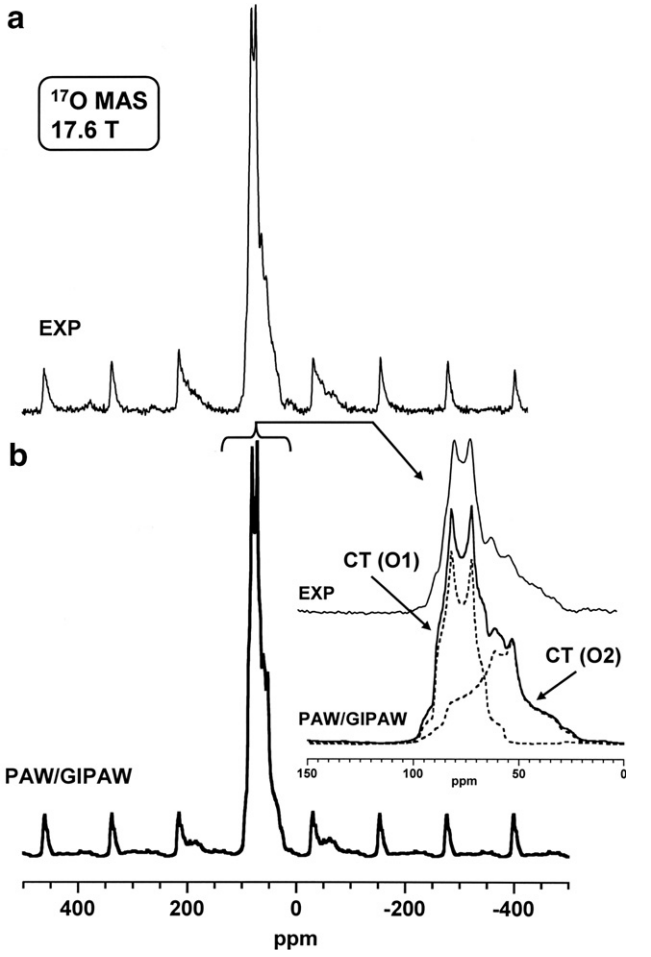

Fig. 4. (a) ^{17}O MAS NMR spectrum (EXP) of $C_6H_5HP^*O(^*OH)$ (LB: 50 Hz) (b) PAW/GIPAW: SIMPSON simulation corresponding to the ^{17}O parameters presented in Table 1. Expansion of the central transitions is also presented (LB used in SIMPSON: 100).

published data concerning the phenyl*phosphonic* acid [5]. However, chemical shift anisotropy values are much higher in the case of the phenyl*phosphinic* acid. This proves that ^{17}O CSA data are very sensitive to molecular structure and must be carefully studied under high field and static conditions, with help of first principles calculations.

We must mention that Bryce et al. [36] have obtained very precise data for ^{17}O EFG, CSA and $^{1}J_{^{17}O-^{31}P}$ tensors for Ph_3PO. In particular, the $^{1}J_{^{17}O-^{31}P}$ value (~150 Hz) was extracted from splitting observed in fast ^{17}O MAS experiments. The present data do not exhibit such splitting. Moreover, static ^{17}O spectra must contain a contribution from *J* and dipolar coupling involving ^{17}O and ^{31}P nuclei. At very high field ($B_0 = 17.6$ T), we assume that CSA acts as the dominant interaction.

The $^{1}H \rightarrow {}^{31}P$ MAS and static spectra are presented in Fig. 6a and b. Using the ^{31}P GIPAW parameters, one obtains good trends for both simulations. One notes however, that the calculated CSA is slightly overestimated, as shown by the static lineshape and the relative intensities of the spinning sidebands in the MAS spectrum. As the

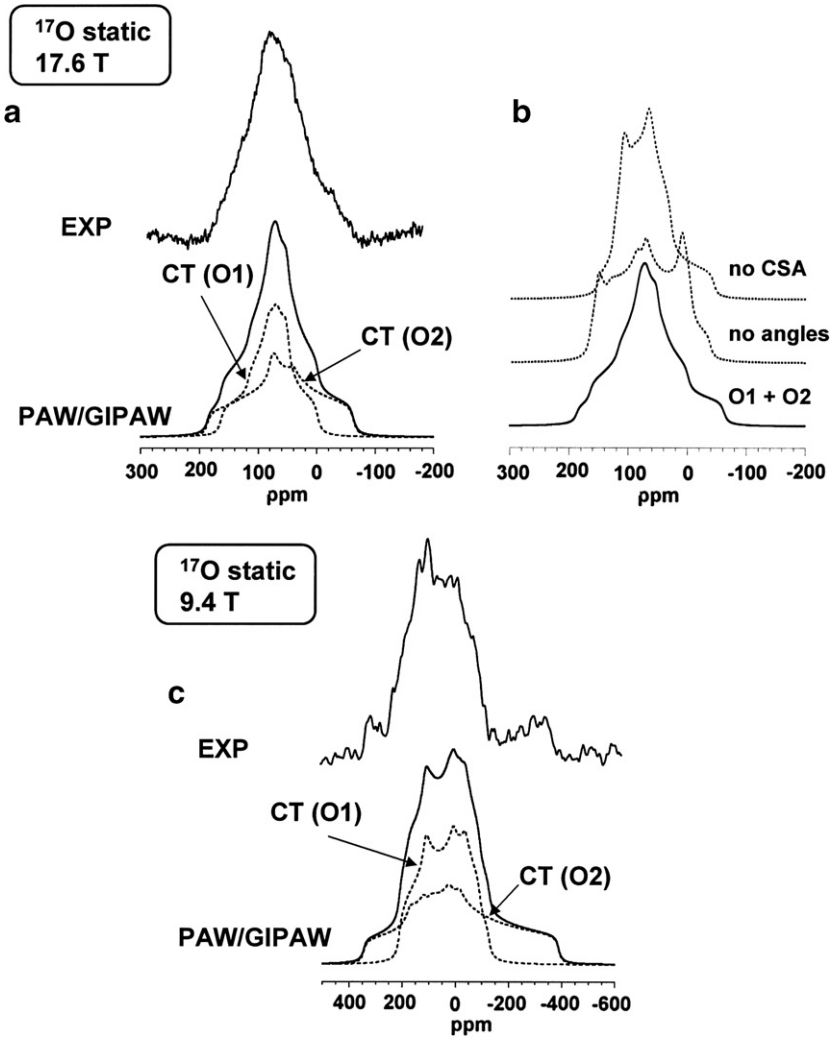

Fig. 5. (a) ^{17}O static NMR spectrum (EXP) of $C_6H_5HP^*O(^*OH)$ at 17.6 T (LB: 100 Hz). PAW/GIPAW: SIMPSON simulation corresponding to the ^{17}O parameters presented in Table 1 (CSA, quadrupolar parameters and Euler angles for O1 and O2). (b) SIMPSON calculations corresponding to O1 and O2 CT's (central transitions) taking into account: the complete set of quadrupolar, CSA parameters and Euler angles shown in Table 1 (O1+O2); quadrupolar, CSA parameters and *coaxial* PAS (no angles); quadrupolar parameters without CSA (no CSA) (LB used in SIMPSON: 1000). (c) ^{17}O static NMR spectrum (EXP) of $C_6H_5HP^*O(^*OH)$ at 9.4 T (LB: 300). PAW/GIPAW: SIMPSON simulation corresponding to the ^{17}O parameters presented in Table 1.

^{31}P–^{1}H direct bond is characterized by a strong dipolar coupling constant (16,100 Hz), the static lineshape will be modulated solely by this particular coupling by using the IRCP local field experiment (for short t_i, Fig. 6c). The P–H distance has been precisely measured by $^{1}H \rightarrow {}^{31}P$ fast MAS experiments [18]. For $t_i = 20$ μs, the most deshielded part of the spectrum is already inverted (Fig. 6d). SIMPSON calculations show that the orientation of the P–H bond (dipolar axis) is parallel to the most deshielded component of the CSA tensor (solid line in Fig. 6d). The dashed line corresponds to a SIMPSON simulation using the GIPAW parameters for the CSA tensor *and* P–H bond direction. Though the lineshape is comparable to the experimental spectrum, the most deshielded part of the line is not inverted.

Starting from the molecular scheme (Fig. 1), one observes that the P–H direction is roughly perpendicular to the calculated δ_{11} principal axis. The deviation from the calculated δ_{33} principal axis is $\Psi \approx 23°$. In the ^{31}P CSA Principal Axes System, the chemical shift corresponding to the P–H direction can be then calculated as a function of δ_{22}, δ_{33} and Ψ. It leads to $\delta = 109.7$ ppm. Surprisingly, this value is similar to the most deshielded component of the *experimental* spectrum (*i.e.* +108.9 ppm). A local movement of the ^{31}P CSA tensor around the P–H bond direction could then account for the slight reduction of CSA (as shown by the static ^{31}P spectrum) and explain why the P–H direction is parallel to the most deshielded CSA component (as shown by the IRCP experiment). Low temperature CP experiment tends to confirm such an assumption. The evolution of the ^{31}P CSA lineshape *vs* T is presented in Fig. 6b. By lowering the temperature, the following trends are observed: the deshielding of the δ_{33} component, the slight shielding of

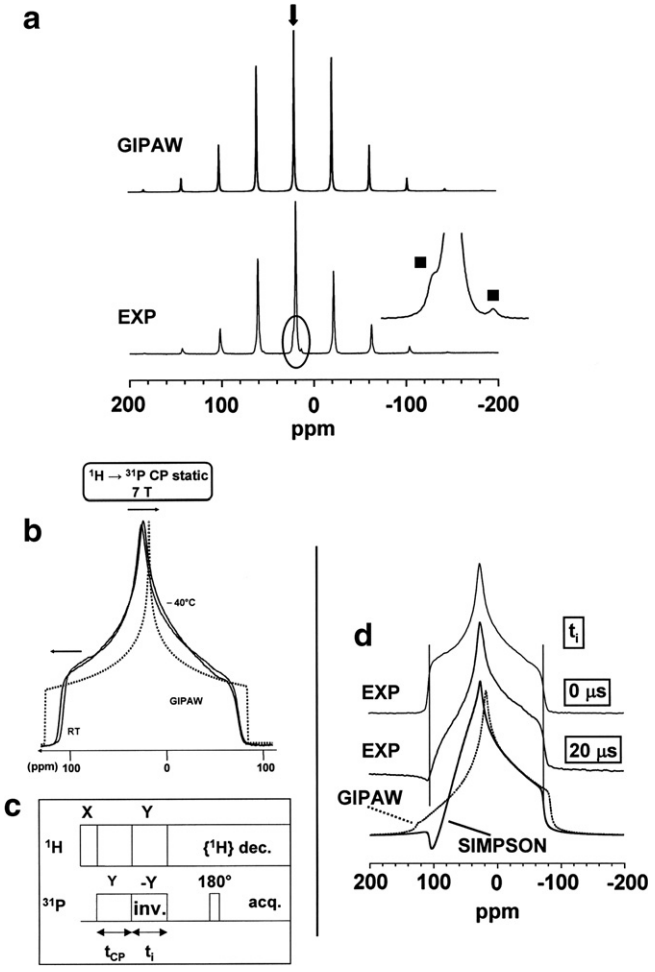

Fig. 6. (a) $^1H \rightarrow {}^{31}P$ CP MAS NMR spectrum (EXP) of $C_6H_5HP^*O(^*OH)$. GIPAW: simulation using the ^{31}P parameters presented in Table 1. ■: satellites due to $^1J_{^{17}O-^{31}P}$. Vertical arrow, isotropic chemical shift. (b) $^1H \rightarrow {}^{31}P$ CP static NMR spectra of $C_6H_5HPO(OH)$. Spectra, room temperature and $T = -40$ °C experiments; GIPAW, simulation using the ^{31}P parameters presented in Table 1. Horizontal arrows, deshielding of δ_{33} and shielding of δ_{22} *vs* T. (c) IRCP sequence [20]. (d) Standard $^1H \rightarrow {}^{31}P$ CP static NMR spectrum ($t_i = 0$ µs) and IRCP static spectrum ($t_i = 20$ µs) of $C_6H_5HPO(OH)$ (EXP) ($B_0 = 7.0$ T). SIMPSON (solid line), simulation of the static IRCP spectrum ($t_i = 20$ µs) using the *experimental* CSA parameters for ^{31}P (see Table 1). GIPAW (dashed line), SIMPSON simulation of the static IRCP spectrum ($t_i = 20$ µs) using the *GIPAW* CSA parameters for ^{31}P (Table 1).

the δ_{22} component and the overall increase of the ^{31}P CSA. The observed low temperature evolution of the CSA principal values is therefore consistent with the GIPAW calculated tensor.

5. Conclusions

By using the PAW/GIPAW approach, full calculation of NMR parameters has been performed in the case of crystalline phenyl*phosphinic* acid $C_6H_5HPO(OH)$. Excellent agreement between calculated and experimental data has been observed for (^1H, ^{13}C, ^{17}O, ^{31}P) CSA parameters, as well as for ^{17}O quadrupolar parameters obtained from ^{17}O enriched $C_6H_5HP^*O(^*OH)$. The analysis of the relative orientation of the CSA and EFG ^{17}O tensors allowed a precise interpretation of the ^{17}O MAS and static spectra at various fields. The role of H-bonding in ^1H solid state NMR was emphasized. In particular, the calculated isotropic chemical shifts of the phenyl*phosphinic* and phenyl*phosphonic* acids were compared to the one calculated for various hydrated calcium phosphates. The deshielding of the chemical shift is clearly related to the shortening of the O<u>H</u>···<u>O</u> distances in the structures. The calculated tensors are generally axial with the unique axes nearly parallel to the OH···O bond directions. The orientation of the P–H bond direction in the ^{31}P CSA PAS was determined by the IRCP sequence. Local reorientation of the CSA tensor is suggested by comparison with the DFT predictions and confirmed by low temperature $^1H \rightarrow {}^{31}P$ CP experiments. A huge amount of work remains to be done for the measurement of ^1H CSA tensors both in terms of magnitude and absolute orientation of the principal axes. First principles calculations should be of great help for the full understanding of such data.

Acknowledgments

Dr D. Massiot is warmly acknowledged for helpful discussions and for the access to the 750 MHz spectrometer in Orléans, France. The calculations have been performed on the IDRIS supercomputer center of the CNRS (Project 51461).

Appendix A. Supplementary data

Supplementary data associated with this article can be found, in the online version, at doi:10.1016/j.jmr.2007.03.018.

References

[1] C.J. Pickard, F. Mauri, All-electron magnetic response with pseudopotentials: NMR chemical shifts, Phys. Rev. B 63 (2001) 245101/1–245101/13.

[2] (a) R.K. Harris, S.A. Joyce, C.J. Pickard, S. Cadars, L. Emsley, Assigning carbon-13 NMR spectra to crystal structures by the INADEQUATE pulse sequence and first principles computation: a case study of two forms of testosterone, Phys. Chem. Chem. Phys. 8 (2006) 137–143;
(b) C. Gervais, R. Dupree, K. Pike, C. Bonhomme, M. Profeta, C.J. Pickard, F. Mauri, Combined first-principles computational and experimental multinuclear solid-state NMR investigation of amino acids, J. Phys. Chem. A 109 (2005) 6960–6969;
(c) J.R. Yates, T.N. Pham, C.J. Pickard, F. Mauri, A.M. Amado, A.M. Gil, S.P. Brown, An investigation of weak CH···O hydrogen bonds in maltose anomers by a combination of calculation and experimental solid-state NMR spectroscopy, J. Am. Chem. Soc. 127 (2005) 10216–10220;
(d) J.R. Yates, C.J. Pickard, M.C. Payne, R. Dupree, M. Profeta, F. Mauri, Theoretical investigation of oxygen-17 NMR shielding and electric field gradients in glutamic acid polymorphs, J. Phys. Chem. A 108 (2004) 6032–6037.

[3] (a) M. Profeta, M. Benoit, F. Mauri, C.J. Pickard, First-principles calculation of the ^{17}O NMR parameters in Ca oxide and Ca aluminosilicates: the partially covalent nature of the Ca–O bond, a

challenge for density functional theory, J. Am. Chem. Soc. 126 (2004) 12628–12635;
(b) E. Balan, F. Mauri, C.J. Pickard, I. Farnan, G. Calas, The aperiodic states of zircon: an ab initio molecular dynamics study, Am. Mineral. 88 (2003) 1769–1777;
(c) T. Charpentier, S. Ispas, M. Profeta, F. Mauri, C.J. Pickard, First-principles calculation of ^{17}O, ^{29}Si, and ^{23}Na NMR spectra of sodium silicate crystals and glasses, J. Phys. Chem. B 108 (2004) 4147–4161;
(d) J.W. Zwanziger, J.L. Shaw, U. Werner-Zwanziger, B.G. Aitken, A neutron scattering and nuclear magnetic resonance study of the structure of GeO_2–P_2O_5 glasses, J. Phys. Chem. B 110 (2006) 20123–20128;
(e) L. Truflandier, M. Paris, C. Payen, F. Boucher, First-principles calculations within periodic boundary conditions of the NMR shielding tensor for a transition metal nucleus in a solid state system: the example of ^{51}V in $AlVO_4$, J. Phys. Chem. B 110 (2006) 21403–21407;
(f) R.T. Hart, J.W. Zwanziger, U. Werner-Zwanziger, J.R. Yates, On the spectral similarity of bridging and nonbridging oxygen in tellurites, J. Phys. Chem. A 109 (2005) 7636–7641.

[4] (a) N. Mifsud, B. Elena, C.J. Pickard, A. Lesage, L. Emsley, Assigning powders to crystal structures by high resolution ^1H-^1H double quantum and ^1H-^{13}C J-INEPT solid-state NMR spectroscopy and first principles computation. A case study of penicillin G, Phys. Chem. Chem. Phys. 8 (2006) 3418–3422;
(b) J.R. Yates, S.E. Dobbins, C.J. Pickard, F. Mauri, P.Y. Ghi, R.K. Harris, A combined first principles computational and solid-state NMR study of a molecular crystal : flurbiprofen, Phys. Chem. Chem. Phys. 7 (2005) 1402–1407.

[5] C. Gervais, M. Profeta, V. Lafond, C. Bonhomme, T. Azaïs, H. Mutin, C.J. Pickard, F. Mauri, F. Babonneau, Combined ab initio computational and experimental multinuclear solid-state magnetic resonance study of phenylphosphonic acid, Magn. Reson. Chem. 42 (2004) 445–452.

[6] F. Pourpoint, C. Gervais, L. Bonhomme-Coury, T. Azaïs, C. Coelho, F. Mauri, B. Alonso, F. Babonneau, C. Bonhomme, Calcium phosphates and hydroxyapatite: solid state NMR experiments and first principles calculations, Appl. Magn. Reson., in press.

[7] (a) M. Mehring, Principles of High Resolution NMR in Solids, Springer Verlag, 1983, pp. 236–240;
(b) U. Haeberlen, Advan. Magn. Res. Supplement, Academic Press, New York, 1976;
(c) U. Haeberlen, U. Kohlschütter, J. Kempf, H.W. Spiess, H. Zimmermann, Proton magnetic shielding in malonic acid by multiple pulse techniques, Chem. Phys. 3 (1974) 248–256.

[8] (a) F. Schönborn, H. Schmitt, H. Zimmermann, U. Haeberlen, C. Corminboeuf, G. Grossmann, T. Heine, The proton nuclear magnetic shielding tensors in biphenyl: experiment and theory, J. Magn. Reson. 175 (2005) 52–64;
(b) T. Heine, C. Corminboeuf, G. Grossmann, U. Haeberlen, Proton magnetic shielding tensors in benzene—from the individual molecule to the crystal, Angew. Chem. Int. Ed. 45 (2006) 7292–7295.

[9] C. McMichael Rohlfing, L.C. Allen, R. Ditchfield, Proton chemical shift tensors in hydrogen-bonded dimers of RCOOH and ROH, J. Chem. Phys. 79 (1983) 4958–4966.

[10] R.A. Haberkorn, R.E. Stark, H. van Willigen, R.G. Griffin, Determination of bond distances and bond angles in solid state nuclear magnetic resonance. Carbon-13 and nitrogen-14 NMR study of glycine, J. Am. Chem. Soc. 103 (1981) 2534–2539.

[11] (a) K. Yamada, S. Dong, G. Wu, Solid-state ^{17}O NMR investigation of the carbonyl oxygen electric-field-gradient tensor and chemical shielding tensor in amides, J. Am. Chem. Soc. 122 (2000) 11602–11609;
(b) G. Wu, S. Dong, R. Ida, N. Reen, A solid-state ^{17}O nuclear magnetic resonance study of nucleic acid bases, J. Am. Chem. Soc. 124 (2002) 1768–1777;
(c) G. Wu, K. Yamada, Determination of the ^{17}O NMR tensors in potassium hydrogen dibenzoate: a salt containing a short O···H···O hydrogen bond, Solid State NMR 24 (2003) 196–208.

[12] (a) K.J. Ooms, K.W. Feindel, V.V. Terskikh, R.E. Wasylishen, Ultrahigh-field NMR spectroscopy of quadrupolar transition metals: ^{55}Mn NMR of several solid manganese carbonyls, Inorg. Chem. 45 (2006) 8492–8499;
(b) M.A.M. Forgeron, R.E. Wasylishen, A solid state ^{95}Mo NMR and computational investigation of dodecahedral and square antiprismatic octacyanomolybdate(IV) anions: is the point-charge approximation an accurate probe of local symmetry? J. Am. Chem. Soc. 128 (2006) 7817–7827;
(c) K.J. Ooms, K.W. Feindel, M.J. Willans, R.E. Wasylishen, J.V. Hanna, K.J. Pike, M.E. Smith, Multiple-magnetic field ^{139}La NMR and density functional theory investigation of the solid lanthanum(III) halides, Solid State NMR 28 (2005) 125–134.

[13] (a) E.R.H. van Eck, M.E. Smith, Orientation of the quadrupole and dipole tensors of hydroxyl groups by ^{17}O quadrupole separated local field NMR, J. Chem. Phys. 108 (1998) 5904–5912;
(b) N.G. Dowell, S.E. Ashbrook, J. McManus, S. Wimperis, Relative orientation of quadrupole tensors from two-dimensional multiple-quantum MAS NMR, J. Am. Chem. Soc. 123 (2001) 8135–8136;
(c) J.D. van Beek, R. Dupree, M.H. Levitt, Symmetry-based recoupling of ^{17}O–^1H spin pairs in magic-angle spinning NMR, J. Magn. Reson. 179 (2006) 38–48.

[14] S. Rossano, F. Mauri, C.J. Pickard, I. Farnan, First-principles calculation of ^{17}O and ^{25}Mg NMR shieldings in MgO at finite temperature: rovibrational effect in solids, J. Phys. Chem. B 109 (2005) 7245–7250.

[15] S. Wi, L. Frydman, Quadrupolar-shielding cross-correlations in solid state nuclear magnetic resonance: detecting antisymmetric components in chemical shift tensors, J. Chem. Phys. 116 (2002) 1551–1561.

[16] (a) G. Guerrero, P.H. Mutin, A. Vioux, Anchoring of phosphonate and phosphinate coupling molecules on titania particles, Chem. Mater. 13 (2001) 4367–4373;
(b) C. Maillet, P. Janvier, M. Pipelier, T. Praveen, Y. Andres, B. Bujoli, Hybrid materials for catalysis? Design of new phosphonate-based supported catalysts for the hydrogenation of ketones under hydrogen pressure, Chem. Mater. 13 (2001) 2879–2884.

[17] G. Guerrero, M. Mehring, P.H. Mutin, F. Dahan, A. Vioux, Syntheses and single-crystal structures of novel soluble phosphonato- and phosphinato-bridged titanium oxo alkoxides, J. Chem. Soc. Dalton Trans. (1999) 1537–1538.

[18] T. Azaïs, L. Bonhomme-Coury, J. Vaissermann, P. Bertani, J. Hirschinger, J. Maquet, C. Bonhomme, Synthesis and characterization of a novel cyclic aluminophosphinate: structure and solid-state NMR study, Inorg. Chem. 41 (2002) 981–988.

[19] V. Lafond, C. Gervais, J. Maquet, D. Prochnow, F. Babonneau, P.H. Mutin, ^{17}O MAS NMR study of the bonding mode of phosphonate coupling molecules in a titanium oxo-alkoxo-phosphonate and in titania-based hybrid materials, Chem. Mater. 15 (2003) 4098–4103.

[20] P. Palmas, P. Tekely, D. Canet, Local-field measurements on powder samples from polarization inversion of the rare-spin magnetization, J. Magn. Reson. A 104 (1993) 26–36.

[21] M. Bak, J.T. Rasmussen, N.C. Nielsen, SIMPSON. A general simulation program for solid-state NMR spectroscopy, J. Magn. Reson. 147 (2000) 296–330.

[22] A.E. Bennet, C.M. Rienstra, M. Auger, K.V. Lakshmi, R.G. Griffin, Heteronuclear decoupling in rotating solids, J. Chem. Phys. 103 (1995) 6951–6958.

[23] A. Bielecki, D.P. Burum, Temperature dependence of ^{207}Pb MAS spectra of solid lead nitrate. An accurate, sensitive thermometer for variable temperature MAS, J. Magn. Reson. A 116 (1995) 215–220.

[24] B. Pfrommer, D. Raczkowski, A. Canning, S.G. Louie, PARATEC (PARAllel Total Energy Code), Lawrence Berkeley National Laboratory, www.nersc.gov/projects/paratec.

[25] R.A. Burrow, D.H. Farrar, A.J. Lough, M.R. Siqueira, F. Squizani, Phenylphosphinic acid, Acta Crystallogr. C56 (2000) e357–e358.

[26] M. Profeta, F. Mauri, C.J. Pickard, Accurate first principles prediction of ^{17}O NMR parameters in SiO_2: assignment of the zeolite ferrierite spectrum, J. Am. Chem. Soc. 125 (2003) 541–548.
[27] P.E. Blöchl, Projector augmented-wave method, Phys. Rev. B 50 (1994) 17953–17979.
[28] H.M. Petrilli, P.E. Blöchl, P. Blaha, K. Schwarz, Electric-field-gradient calculations using the projector augmented wave method, Phys. Rev. B 57 (1998) 14960–14967.
[29] D. Massiot, F. Fayon, M. Capron, I. King, S. Le Calvé, B. Alonso, J.O. Durand, B. Bujoli, Z. Gan, G. Hoatson, Modeling one- and two-dimensional solid-state NMR spectra, Magn. Reson. Chem. 20 (2002) 70–76.
[30] I. Schnell, H.W. Spiess, High-resolution ^{1}H NMR spectroscopy in the solid state. Very fast sample rotation and multiple-quantum coherences, J. Magn. Reson. 151 (2001) 153–227.
[31] B. Berglund, R.W. Vaughan, Correlations between proton chemical shifts tensors, deuterium quadrupole couplings, and bond distances for hydrogen bonds in solids, J. Chem. Phys. 73 (1980) 2037–2043.
[32] G.A. Jeffrey, Y. Yeon, The correlation between hydrogen-bond lengths and proton chemical shifts in crystals, Acta Crystallogr. B42 (1986) 410–413.
[33] G. Wu, C.J. Freure, E. Verdurand, Proton chemical shift tensors and hydrogen bond geometry: a ^{1}H–^{2}H dipolar NMR study of the water molecule in crystalline hydrates, J. Am. Chem. Soc. 120 (1998) 13187–13193.
[34] C. Bonhomme, C. Coelho, T. Azaïs, L. Bonhomme-Coury, F. Babonneau, J. Maquet, R. Thouvenot, Some triple resonance experiments in solid-state CP MAS NMR: $^{51}V/^{29}Si$, $^{31}P/^{13}C$, and $^{29}Si/^{13}C$, C. R. Chimie 9 (2005) 466–471.
[35] B.F. Chmelka, J.W. ZwanzigerNMR Basic Principles and Progress, vol. 33, Springer Verlag, 1994.
[36] D.L. Bryce, K. Eichele, R.E. Wasylishen, An ^{17}O NMR and quantum chemical study of monoclinic and orthorhombic polymorphs of triphenylphosphine oxide, Inorg. Chem. 42 (2003) 5085–5096.
[37] J.C. Elliot, P.E. Mackie, R.A. Young, Monoclinic hydroxyapatite, Science 180 (1973) 1055–1057.